

ANISOTROPIC INVERSE COMPTON SCATTERING IN GAMMA-RAY BINARIES

B. Cerutti¹, G. Dubus¹ and G. Henri¹

Abstract.

Amongst the 40 TeV sources discovered by HESS and MAGIC experiments, three have been identified as gamma-ray binaries : LS 5039, LS I +61°303 and PSR B1259-63. Because of the relative position of the compact object, the companion star and the observer, the spectrum of very high energy photons emitted by inverse Compton scattering on stellar photons will depend on the orbital phase. We investigate the effect of this anisotropy on the spectra and lightcurves, focusing on LS 5039. The latter is composed of a compact object and a massive O6.5V star in a 3.9 day eccentric orbit. Observations of this binary have been carried out by HESS in 2004-2005 and revealed an orbital modulation in the TeV gamma-ray flux and spectrum.

1 Introduction

Gamma-ray binaries have been established in the past couple of years as a new class of very high energy (VHE, >100 GeV) photons. They are characterized by a large gamma-ray luminosity above MeV, at the level or exceeding their X-ray luminosity. Today amongst the 40 TeV sources discovered by HESS and MAGIC experiments, three have been identified as gamma-ray binaries : LS 5039 (Aharonian et al. 2005a), LS I+61°303 (Albert et al. 2006) and PSR B1259-63 (Aharonian et al. 2005b), recently possibly joined by Cyg X-1 (Albert et al. 2007). These systems are composed of a massive Be or O star and a compact object in an eccentric orbit situated between 1.5 to 3 kpc. In PSR B1259-63, the compact object is a young 48 ms radio pulsar. The VHE emission arises from the interaction of the relativistic wind from the pulsar, extracting rotational energy from the neutron star, with the stellar wind from its companion. At the shock between the two winds, particles are accelerated and radiate VHE. This is the PWN (Pulsar Wind Nebula) scenario imagined by Maraschi & Treves (1981) and applied to LS I+61°303. The nature of the compact object and origin of the VHE emission are still controversial in LS 5039 and LS I+61°303. However, spectral and temporal similarities between the three binaries suggest that they are actually all composed of a young pulsar (Dubus 2006b, 2007). Alternatively, the VHE emission could originate from particles accelerated in a relativistic jet, the energy source being the accretion onto a black hole or neutron star. In both scenarios, VHE gamma-rays are produced by accelerated particles to high energies. If particles are leptons, the only viable gamma-ray radiation mechanism is inverse Compton scattering on the stellar photons. Because of the relative position of the compact object, the companion star and the observer, the VHE spectrum emitted by inverse Compton scattering on stellar photons will depend on the orbital phase. We investigate the effect of this anisotropy on the spectra and lightcurves, adopting the PWN scenario and focusing on LS 5039.

2 Anisotropic inverse Compton scattering

2.1 Basic equations and kernel

The principle of inverse Compton calculations are simple and can be divided into two steps. First, the scattering is studied in the rest frame of the electron and standard equations of the Compton scattering are considered. Once the equations are written, they are expressed in the observer frame. Quantities in the electron frame are primed and quantities in the observer frame are left unprimed. Relativistic kinematics links the energy of the

¹ Laboratoire d'Astrophysique de Grenoble, UMR 5571 CNRS, Université Joseph Fourier, BP 53, 38041 Grenoble, France

scattered photon ϵ'_1 to the energy of the incoming (stellar) photon ϵ'_0 and the electron mass m_e by the Compton formula

$$\epsilon'_1 = \frac{\epsilon'_0}{1 + \frac{\epsilon'_0}{m_e c^2} (1 - \cos \Theta')} \quad (2.1)$$

with Θ' the angle between the incoming and the outgoing photons. Quantum ElectroDynamics leads to the probability of interaction between the incoming photon and an electron. The differential cross-section in the electron rest frame is given by the Klein-Nishina formula

$$\frac{d\sigma}{d\epsilon'_1 d\Omega'_1}(\epsilon'_0, \epsilon'_1, \Theta') = \frac{r_e^2}{2} \left(\frac{\epsilon'_1}{\epsilon'_0}\right)^2 \left(\frac{\epsilon'_1}{\epsilon'_0} + \frac{\epsilon'_0}{\epsilon'_1} - \sin^2 \Theta'\right) \delta\left(\epsilon'_1 - \frac{\epsilon'_0}{1 + \frac{\epsilon'_0}{m_e c^2} (1 - \cos \Theta')}\right) \quad (2.2)$$

where r_e^2 is the classical electron radius and δ the Dirac distribution. In the simple case of a monoenergetic beam of photons scattering off a single electron, it is possible to perform analytical calculations. The fraction of photons scattered per unit of time, energy and solid angle in the electron rest frame is (Jones 1968; Blumenthal & Gould 1970)

$$\frac{dN'}{dt' d\epsilon'_1 d\Omega'_1} = \int \int c \frac{d\sigma}{d\epsilon'_1 d\Omega'_1} \frac{dn'}{d\epsilon' d\Omega'} d\Omega' d\epsilon' \quad (2.3)$$

where $\frac{dn'}{d\epsilon' d\Omega'}$ is the incoming photon density. The useful quantity is the number of photons scattered per electron, per unit of time and energy $\frac{dN}{dt d\epsilon_1}$ in the observer frame. This quantity is known as the fundamental kernel. It is a convenient tool containing all the physical properties of inverse Compton scattering and adaptable to any astrophysical problem.

2.2 Kernel for spectral calculations

The Compton kernel can be used for spectral calculations in any astrophysical systems. In that case, it is important to take into account the physical properties of the problem: the incoming photon density, the radiating electrons density and the geometric parameters of the considered system. The total spectrum in photons $\text{s}^{-1}\text{erg}^{-1}\text{sr}^{-1}$ is

$$\frac{dN_{tot}}{dt d\epsilon_1 d\Omega_1} = \int \int \int \int \frac{dN}{dt d\epsilon_1 d\Omega_1} n_0 d\Omega_0 d\epsilon_0 \frac{dn_e}{d\gamma_e d\Omega_e} d\Omega_e d\gamma_e \quad (2.4)$$

with $\frac{dn_e}{d\gamma_e d\Omega_e}$ and n_0 the electrons respectively photons densities.

2.3 Anisotropic scattering of stellar photons: a simple example

Figure 1 shows computed spectra from a distribution of relativistic electrons scattering photons emitted by a star, for different viewing angles. The incoming photons have a blackbody distribution and the electrons have an isotropic power-law distribution. The viewing angle is defined as the angle between the star, electron cloud and observer. The orbit is assumed circular and seen with an inclination $i = 90^\circ$. On the left panel, the electrons energies are small enough to consider the elastic Thomson scattering approximation in the electron rest frame. On the right panel, the electrons energies are much greater and Klein-Nishina effects become significant and the flux decreases at VHE. In both cases, the inverse Compton flux exhibits a strong dependance on the viewing angle. The decrease of the emitted flux and the shift to higher energies of the Klein-Nishina effects for small angles are due to the $1 - \beta \cos \psi$ term in the Lorentz transform.

3 Application to LS 5039

LS 5039 presents an ideal testbed for the anisotropic inverse Compton emission in the PWN scenario. The massive star has an O6.5V spectrum ($T_* = 39000 \text{ K}$, $R_* = 9.3 R_\odot$, $M_* = 23 M_\odot$) in a 3.9 day eccentric orbit ($e=0.35$) with its compact companion (Casares et al. 2005). The measured radial velocity of the O star constraints the inclination to about 60° for a neutron star companion and less than about 20° for a black hole. The neutron star scenario is discussed below.

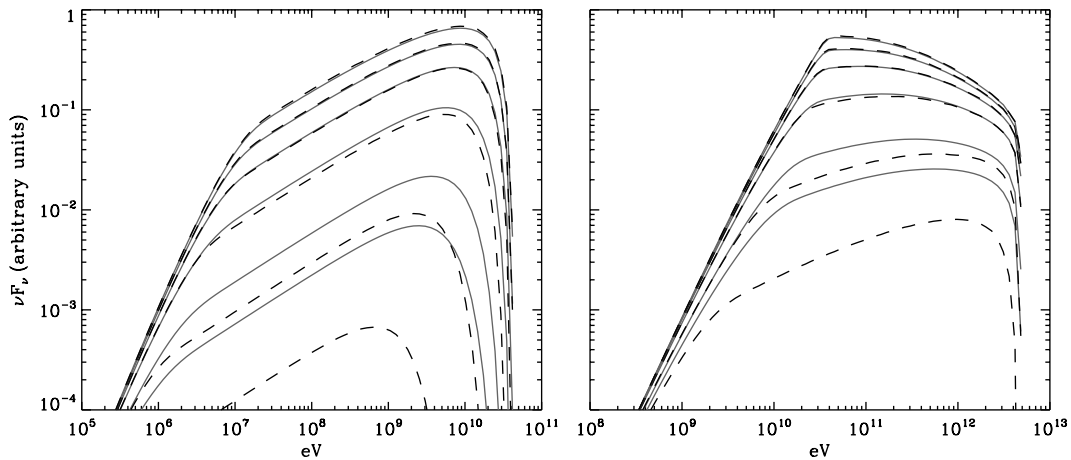


Fig. 1. Dependence of the viewing angle on the inverse Compton spectrum (15° (bottom), 30° , 60° , 90° , 120° and 180° (top)). Photons are from a star with $kT = 1$ eV, the electron cloud is situated at a distance $d = 2R_*$ following a power law distribution $\propto \gamma_e^{-2}$. Left panel: $10^3 < \gamma_e < 10^5$, right panel: $10^5 < \gamma_e < 10^7$. Dashed lines correspond to the point source approximation.

3.1 The radiating electrons

In the emitting zone, assumed to be close to the compact object, electrons cool down via synchrotron and inverse Compton losses. If the injection of particles is constant, the considered emitting electron distribution is steady-state. At low energy, inverse Compton losses dominate until synchrotron losses become greater at VHE ($\gamma_e > \gamma_{brk}$), depending on the magnetic field. Assuming a power law injection spectrum $\propto \gamma_e^{-2}$, synchrotron and inverse Compton losses in the Thomson regime steepen the electron spectrum to γ_e^{-3} . Inverse Compton losses in the Klein-Nishina regime decrease due to the drop of the cross section, producing a harder spectrum between γ_{kn} and γ_{brk} . Simple considerations on cooling timescales and using a full numerical calculation, the steady-state distribution of the radiating electrons is obtained and presented in figure 2 (see also Moderski et al. 2005; Dubus 2006b). These timescales are very small compared to the orbital timescale so the steady-state approximation is justified at VHE.

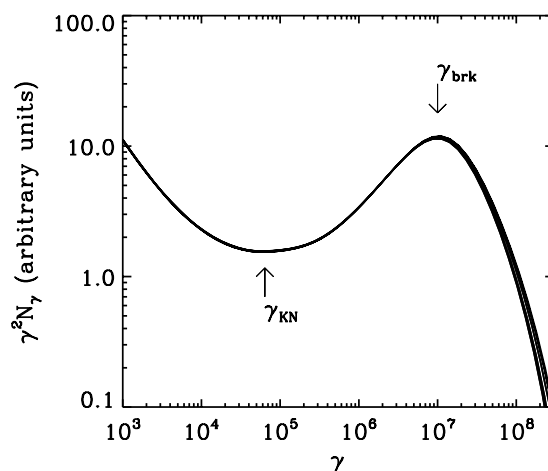


Fig. 2. Steady-state electron distribution N_e along the orbit of LS 5039. A power-law γ_e^{-2} with an exponential cut-off at $\gamma_e \approx 10^8$ was used for the injection spectrum. Inverse Compton and synchrotron losses steepen the injected distribution to $N_e \propto \gamma_e^{-3}$ except in the Klein-Nishina regime between γ_{kn} and γ_{brk} where the distribution is harder.

3.2 Orbital lightcurve

When all the parameters of the system are taken into account, it is possible to compute the theoretical lightcurve expected with the model. Figure 3 (left panel) shows the computed lightcurves, taking into account the absorption $\gamma - \gamma$ occurring in gamma-ray binaries (Dubus 2006a). The flux is modulated by the distance to the star due to the orbital eccentricity, the anisotropy in the emission and by absorption. The lightcurve including both anisotropic emission and attenuation by pair production reproduces very well the observed lightcurve (Aharonian et al. 2006). Most notably, the combination of low attenuation, increasing photon density and a hard inverse Compton spectrum produces a small peak after inferior conjunction that appears to be present in the HESS observations. This peak is a key feature of this model.

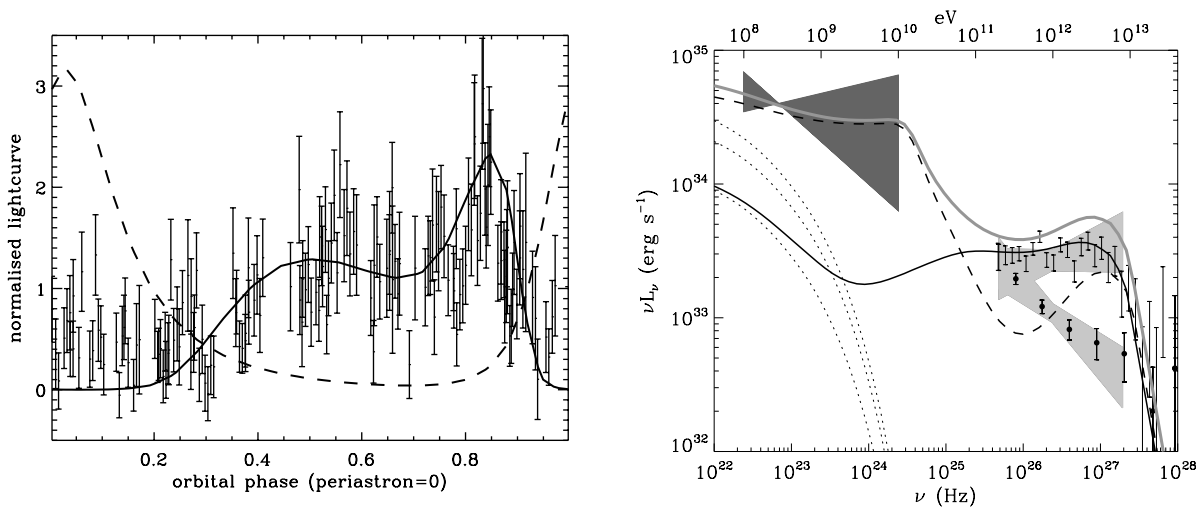


Fig. 3. Left panel: Predicted orbital lightcurves for LS 5039 in the case of a neutron star ($i = 60^\circ$), HESS lightcurve Flux > 1 TeV (solid line, experimental data), GLAST lightcurve Flux > 1 GeV (dashed line). **Right panel:** Comparison with the EGRET (dark grey bowtie) and HESS observations (light grey bowtie) of the LS 5039 model spectra for a neutron star. In this figure are plotted: the high state (black solid line), the low state (black dashed line), the synchrotron spectra (dot lines) and the total spectrum (grey solid line).

3.3 Phase-resolved spectra

HESS observations revealed two spectral states for LS 5039 (Aharonian et al. 2006): a ‘low’ state when the compact object is in the back ($\phi_{orb} < 0.45$ or $\phi_{orb} > 0.9$) and a ‘high’ state when it is in the front of the companion star ($0.45 < \phi_{orb} < 0.9$). It is worthwhile to look at the predicted spectra from this simple model. Figure 3 (right panel) shows the predicted two spectra and are compared to the experimental data (HESS and EGRET). The high state fits particularly well and enables to put strong constraints on the system compatible with the lightcurve. The VHE cut-off constraints the magnetic field to $B = 0.8 \pm 0.2$ G at periastron, the slope gives an injection spectrum slope at $p = 2 \pm 0.3$ and the normalized intensity gives the total energy contained in the electrons $E_{tot} = 3 \cdot 10^{37}$ erg.

4 Conclusion

The anisotropic behaviour of inverse Compton scattering has a major influence on the emission from gamma-ray binaries. The LS 5039 lightcurve and spectra were modelled using a simple-minded leptonic model. The combination of absorption, orbital parameters and anisotropy in the emission enables to do prediction on GLAST lightcurve and to put strong constraints on the system. These results confirm that gamma-ray binaries are promising sources to study the environment of pulsars on very small scales.

References

- Aharonian, F.A., et al. (HESS collaboration), 2005a, *Science*, 309, 746
- Aharonian, F.A., et al. (HESS collaboration), 2005b, *A&A*, 442, 1
- Aharonian, F.A., et al. (HESS collaboration), 2006, *A&A*, 460, 743
- Albert, J., et al. (MAGIC collaboration), 2006, *Science*, 312, 1771
- Albert, J., et al. (MAGIC collaboration), 2007, *ApJ*, 665, L51
- Blumenthal, G.R., Gould, R.J., 1970, *Reviews of Modern Physics*, 42, 237
- Casares, J., Ribó, M., Ribas, I., et al., 2005, *MNRAS*, 364, 899
- Dubus, G., 2006a, *A&A*, 451, 9
- Dubus, G., 2006b, *A&A*, 456, 801
- Dubus, G., 2007, *AIP Conference Proceedings*, 921, 65 (arXiv:0704.0536)
- Jones, F.C., 1968, *Physical Review*, 167, 1159
- Maraschi, L., and Treves, A., 1981, *MNRAS*, 194, 1L
- Moderski, R., Sikora, M., Coppi, P.S., Aharonian, F., 2005, *MNRAS*, 363, 954